Journal of Food Engineering 195 (2017) 61–72

Contents lists available at ScienceDirect

Journal of Food Engineering

journal homepage: www.elsevier.com/locate/jfoodeng

Rheological measurements for characterizing sticky point temperature of selected fruit powders: An experimental investigation

O.A. Caparino [a], C.I. Nindo [b, *], J. Tang [c], S.S. Sablani [c]

[a] Philippine Center for Postharvest Development and Mechanization (PHilMech), Science City of Munoz, Nueva Ecija 3120, Philippines
[b] Center for Food Science & Technology, University of Maryland Eastern Shore, Princess Anne, MD 21853, USA
[c] Biological Systems Engineering Department, Washington State University, Pullman, WA 99164-6120, USA

ARTICLE INFO

Article history:
Received 11 May 2016
Received in revised form
15 August 2016
Accepted 7 September 2016
Available online 14 September 2016

Keywords:
Characterization
Sticky point temperature
Model fruit powder
Sugar-rich food powders
Rheometer
Drying
Pasteurization

ABSTRACT

Stickiness is one of the common problems frequently encountered during production, handling and storage of fruit powders with high concentration of low molecular weight sugars. Several techniques and devices were developed in the past to determine the level of stickiness of some of those products. Nevertheless, there is still a need for a simple, more accurate and reliable method. In this study, a new method to quantify and characterize the sticky point temperature (T_s) of fruit powder was explored using a rheometer technique. The rheometer system utilized a serrated parallel plate to hold the samples and was operated in dynamic oscillation mode at a frequency of 1 Hz and a constant strain amplitude of 2%. The samples of a model fruit powder (Refractance Window (RW)-dried mango powder) were scanned from 25 to 95 °C at an increment of 10 °C and a holding time of 180 s for each increment. A *crossover* between the storage modulus (G') and loss modulus (G'') was established and denoted as sticky point temperature of the model fruit powder. Results showed that the sticky point temperature obtained using the new method agreed well with the published data and can be considered as a suitable technique to characterize the sticky point temperature of sugar-rich materials. The procedure for sample conditioning and rheometric measurements to determine the sticky point temperature are straightforward. This new technique can measure the sticky point temperature of fruit powders with a high degree of repeatability and accuracy (SD = 0.58–1.73 °C).

1. Introduction

Stickiness is a major quality index for food powders in traditional food processing operations such as drying, handling, storage, and is also a concern for equipment cleaning and sanitation. Recent academic and industrial interest in thermal pasteurization of low moisture foods to control Salmonella spp., *Cronobacter* spp., and other pathogens (Villa-Rojas et al., 2013) make the study of quality changes in powder products after heat treatments even more relevant. Likewise, stickiness is frequently encountered in food powders with high concentration of low molecular weight sugars, e.g. glucose, fructose and sucrose (Downton et al., 1982; Bhandari et al., 1997). Schubert (1987) reported that the mechanisms that may influence the tendency of particles to stick together include liquid bridging, solid bridging, inter-particle attraction forces and mechanical attraction. Liquid bridging happens when a sufficient amount of moisture is present between particles, while solid bridging is a result of solid diffusion or condensation within the solid matrix, normally at elevated temperatures (Barbosa-Canovas et al., 2005). The appearance of liquid bridges between powder particles allows for the transformation of the material from the glassy to rubbery phase and greatly influences its strength, causing it to be sticky (Ozkan et al., 2002).

Stickiness of materials in amorphous form is also due to water plasticization and its subsequent depression of glass transition temperature during processing and storage (Goula et al., 2007). Thus, stickiness of amorphous materials is influenced by its glass transition temperature. Roos (1993) reported that the sticky point temperature (T_s) of sugars is higher than the glass transition temperature (T_g) at $T_s - T_g$ between 10 and 20 °C. If the temperature of a glassy amorphous material exceeds T_g, then the material is transformed into a rubbery state and may become sticky Roos and Karel (1991a). This implies that stickiness can be prevented if the

* Corresponding author. 2127 Center for Food Science & Technology, University of Maryland Eastern Shore, Princess Anne, MD 21853, USA.
E-mail address: cinindo@umes.edu (C.I. Nindo).

http://dx.doi.org/10.1016/j.jfoodeng.2016.09.010
0260-8774/

temperature of amorphous material is kept below T_g. Previous experiments on tomato, pineapple and mango powders (Jaya and Das, 2009), and milk powder (Hennigs et al., 2001) showed that T_s and T_g change with moisture content, but the difference between the two temperatures ($T_s - T_g$) was constant at a given water content.

The transformation of glassy amorphous material to rubbery state was associated with the storage modulus (G') and loss modulus (G'') (Rao, 1999). The G' value is a measure of deformation energy stored in the samples during the shear process (elastic behavior), while G'' is a measure of dissipation of energy (viscous behavior) (Mezger, 2006). It has been reported that when the material is in a glassy solid form, the value of G' is expected to be higher than G'', while the materials are transformed into rubbery state or become "liquid-like" when G'' exceeds G' (Rao, 1999). Using the mechanism of liquid-bridging related to elasticity and viscous behavior of the material at the interface, the observed values wherein G' and G'' are crossing at certain temperature can also be characterized as sticky point temperature of powder as a function of water activity and water content.

Several direct techniques to characterize the stickiness of food products have been reported. The oldest published method is the manually-driven propeller method initially developed by Lazar et al. (1956) to measure T_s of spray-dried tomato, orange, mango, and other powders. Brennan et al. (1971) modified the Lazar design by adding a motor-driven impeller, which Hennigs et al. (2001) further improved by connecting the impeller to a data logging system to record electrical resistance output. Ozkan et al. (2002) developed a rotational viscometry technique with an L-shape spindle inserted into the powder to measure T_s. The torque required to rotate the spindle at a given temperature is recorded using a data logging system connected to the viscometer. Kudra and Mujumdar (2002) also reported a semi-automatic sticky-point tester with humidity control. Adhikari et al. (2003) developed an *in situ* method for measuring sticky point temperature consisting of a drying chamber, an image acquisition system and a weighing balance connected to a data logging device. There are other methods reported in the literature, such as the Jenike shear cell method (Jenike, 1964), ampule method (Tsourouflis et al., 1976), fluidization test (Dixon et al., 1999), blow test (Paterson et al., 2001), cyclone sticky test (Boonyai et al., 2004), tack method (Green, 1941), and the contact probe test method (Kilcast and Roberts, 1998; Adhikari et al., 2001, 2003).

However, a critical analysis conducted by Boonyai et al. (2004) suggests that the above measuring devices and techniques are all empirical in nature. They also noted that due to the inaccuracy and difficulty of application of these devices to actual processing and handling operations, there are continuing demands and challenges to develop accurate, simple and easy to use methods to characterize the onset of stickiness of selected food powders. This research was carried out to develop and investigate a new method to quantify and characterize the sticky point temperature (T_s) of fruit powder using a rheometer technique.

2. Materials and methods

2.1. Preparation of samples

Refractance Window® (RW)-dried mango powder was chosen as the model sample for the entire experiment. The powder with water content of 0.039 kg water/kg dry solids was produced using the RW drying process following the procedure described by Caparino et al. (2012). One hundred grams of RW-dried mango powder with particle size ranging from 180 to 350 μm was prepared by slight grinding using a mortar and pestle, and sieving using mesh sizes of 80 and 45 (American Society for Testing and Materials, ASTM) (Barbosa-Canovas et al., 2005). The particle size range selected was based on the approximate size of the serration of the two parallel plate geometries used during the sticky point measurements. The prepared powder samples were put inside aluminum-coated polyethylene bags, flushed with nitrogen gas, heat sealed and kept at −35 °C for use in later measurements.

2.2. Conditioning of samples at different water content

Overall, samples with six different water contents (0.003, 0.022, 0.029, 0.039, 0.048, and 0.066 kg water/kg dry solids) were prepared and used in the experiment. The conditioning of samples was carried out by drying or by water absorption methods. The prepared RW-dried mango powders with water content of 0.039 kg water/kg dry solids served as the starting reference sample prior to conditioning. The samples with water content below 0.039 kg water/kg dry solids were obtained by drying the reference sample, while those above 0.039 kg water/kg dry solids were prepared by conditioning in thin-layers under 100% relative humidity for different times. The sample with water content of 0.003 kg water/kg dry solids was achieved by putting 5 g of the reference sample in a sealed jar containing P_2O_5 solution to avoid mold development and storing for 30 days at room temperature.

The samples with water content of 0.022 and 0.029 kg water/kg dry solids were obtained by placing 2 g of the reference sample in an aluminum pan with approximate thickness of 1 mm and oven-dried at 50 °C for 30 and 60 min, respectively. To obtain samples with higher water contents of 0.048 and 0.067 kg water/kg dry solids, the reference samples were spread in a 90 mm diameter Whatman #2 filter paper and placed on top of a perforated membrane located 20 mm above the water level inside a sealed container (Polylab® Plasticware, Hyderabad, India) and held for 20 and 40 min at room temperature, respectively. The relative humidity inside the container was assumed to be ~100%. To obtain uniform moisture adsorption during conditioning at ~100% RH, an aluminum sample holder with a dimension of 2 × 2 inch and thickness of 2 mm was fabricated. The size of the holder allowed spreading of samples evenly to 2 mm thickness onto the filter paper prior to loading into the desiccator to equilibrate. Apparently, the powder formed a lump of particles or agglomerated after conditioning at ~100% RH, and hence they were dispersed quickly using a stainless spatula, sealed in a small bottle and kept at room temperature for at least 2 h to equilibrate prior to measurement and analysis. Mango powder with water content greater than 0.067 kg water/kg dry solids were not included in the measurement because the material became very sticky at room temperature and were no longer practical to use for the study. We note here that some researchers were able to measure the sticky point temperature of a material up to 0.08 kg water/kg dry solids for higher molecular weight samples such as mango, orange and pineapple powders with added maltodextrin carrier (Jaya and Das, 2009).

2.3. Determination of water content

Water content of mango powder samples was determined using an automatic Karl Fischer titrator (Mettler Toledo, Columbus, OH) following the procedure in the instrument manual. Approximately 1 g of mango powder was put into the titration vessel through a funnel with the aid of a glossy paper. The exact sample weight was measured to 0.1 mg accuracy before delivering the same into the titration vessel. Following titration, the water content was determined automatically via a built-in software program. Measurements were performed in triplicate at room temperature.

2.4. Characterization of sticky point temperature using the rheological method

2.4.1. Rheometer system and loading process

The sticky point temperature measurement was performed using AR2000 controlled stress – controlled rate advanced rheometer (TA Instruments, New Castle, DE). The rheometer system was fitted with a lower and upper stainless serrated plate with a diameter of 65 mm and 20 mm, respectively (Fig. 1a). The lower plate was fixed directly above the Peltier plate (heating/cooling system that controls the test material temperature), while the upper plate was free to oscillate with no supplemental heating. The serrated 'groove' parallel plate geometry was selected as a design criterion to prevent slippage between particles and the parallel plate during oscillation, and to minimize moisture evaporation from the samples during the experiment. A roughened or serrated

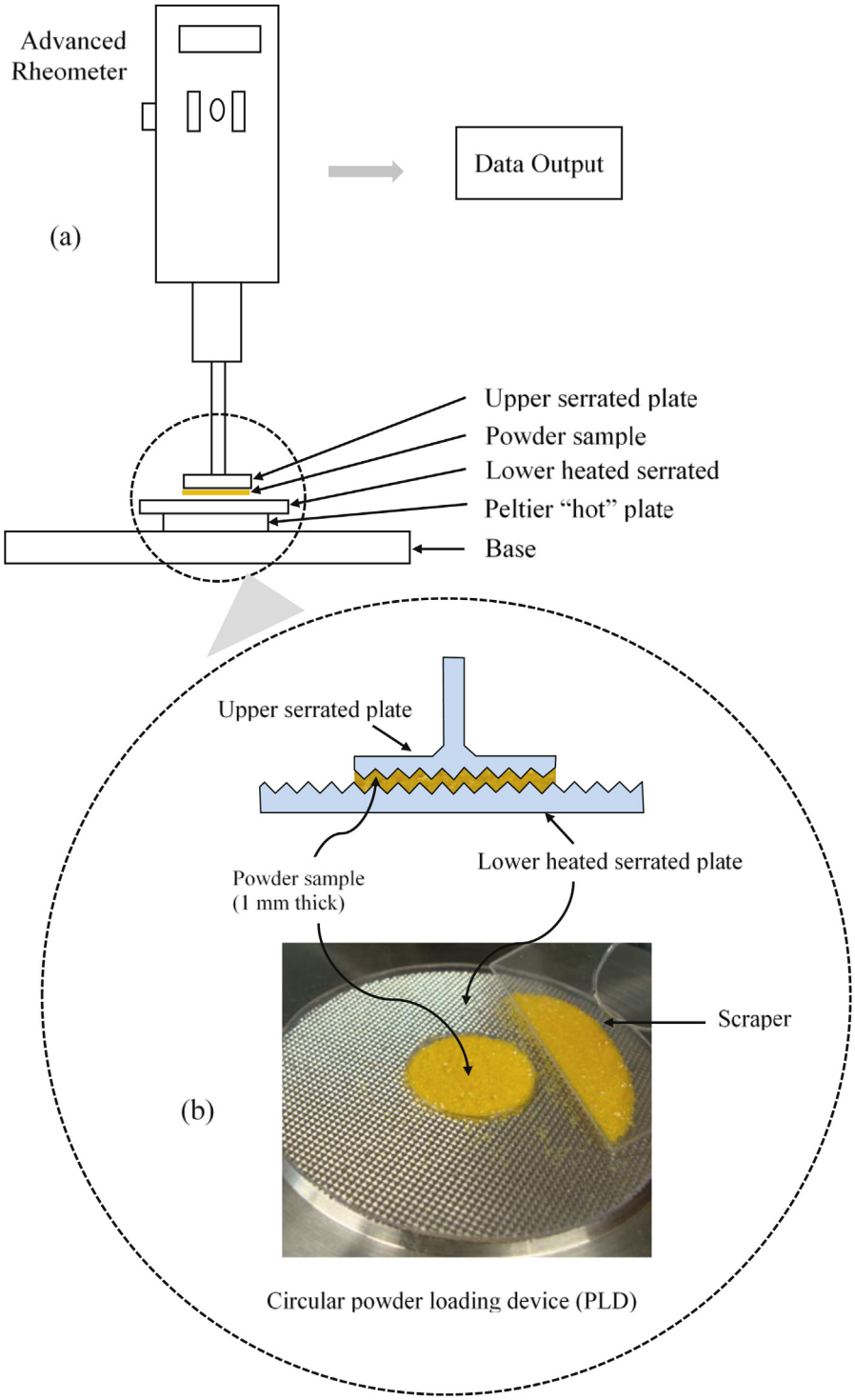

Fig. 1. Schematic diagram of (a) rheometer system, and (b) loading process of mango powder.

surface plate was reported to be effective in preventing slippage in oscillatory testing of cookies and crackers dough (Menjivar and Faridi, 1994). The temperature and moduli responses were continuously monitored via instrument sensors connected to a computer equipped with proprietary control software.

2.4.2. Loading of samples

A circular powder loading device (PLD) made from polycarbonate material was fabricated (Fig. 1b). The PLD with an outside diameter of 65 mm and central hole of 20 mm was positioned at the center of the serrated lower plate of the rheometer. Approximately 300 mg of mango powder with particle sizes ranging from 180 to 350 μm was poured to fill the circular hole of the PLD, using a stainless spatula, followed by carefully scraping the excess material (without tapping) with the aid of a straight-fine edge cut polycarbonate material. After scraping, the PLD was removed by first holding the side portion of the loader while gently lifting the other side in a slightly inclined motion, leaving a circular-molded shape of the powders with a 20 mm diameter and 1 mm thickness.

2.4.3. Rheological settings and measurements

Rheometric measurement was carried out immediately after loading the samples and covering with a solvent trap to minimize sample moisture changes during the test. The rheometer was operated in dynamic oscillation mode with a 1 mm gap between the parallel plate geometries (upper and lower plate). A time sweep dynamic test for the model sample was applied at a frequency of 1 Hz and a constant strain amplitude of 2%. Samples with different water content were exposed to varying temperatures by ramping from 25 to 95 °C in steps of 10 °C. This step temperature ramp procedure, at in-built machine ramp rate to the next level, was adopted because our preliminary experiment on continuous scanning at 3, 5 and 10 °C/min resulted in a delayed temperature response and a non-reproducible output. To ensure that the temperature readings represented the actual conditions, the samples were held constant for 180 s at each temperature, generating 20 data points before ramping to the next higher temperature level. We did not do physical measurement of temperature variation within the loaded bulk powders due to difficulty of inserting temperature sensors inside the 1 mm gap between the parallel plates. However, considering that the thickness of the powders was only 1 mm and the estimated amount of powders lodged in each serration of the two parallel plates was less than 2 mg, the temperature gradient in all sections of the loaded samples during heating was assumed to be insignificant. Also, due to the very high heat capacity and heat transfer coefficient of the serrated stainless steel plates, the temperatures recorded were assumed to be the same as sample temperature.

Two sticky point temperatures measured in the proposed method were denoted as the end-point sticky point temperature (T_{se}) and average sticky point temperature (T_{sa}). T_{se} for each temperature setting were obtained from the end-point value during a holding time of 180 s during ramping, while T_{sa} was taken from the average of 20 data points recorded during the holding time period. The measured sticky point temperatures at different water content were used to establish a “sticky-point curve”. All measurements were performed in triplicate at room temperature.

2.5. Measurement of glass transition temperature

Previous studies comparing sticky point temperature and glass transition temperature (T_g) of sugar-rich materials showed a linear direct relationship with almost parallel trend ($T_s - T_g$) at different water content (Jaya and Das, 2009; Downton et al., 1982). Thus, determination of T_g for the current investigation was also carried out to confirm this relationship. The T_g of RW-dried mango powders with different water content levels (0.003, 0.022, 0.029, 0.039, 0.048 and 0.067 kg water/kg dry solids) was measured using a Q2000 differential scanning calorimeter (TA Instruments, New Castle, DE) following the procedure described by Syamaladevi et al. (2009). The calorimeter was calibrated for heat flow and temperature using indium and sapphire standards. Twelve to 14 mg of each mango powder sample was sealed in an aluminum pan (volume of 30 μl), cooled down from 25 °C to −90 °C using liquid nitrogen and then equilibrated for 10 min. The samples at −90 °C were scanned to 90 °C and then cooled down to 25 °C. Scanning of all samples was carried out at 5 °C/min for both heating and cooling. The reversing and non-reversing components of the total heat flow curves was monitored in preliminary tests, but high instrument sensitivity allowed the T_g to be identified from total heat flow after the initial cooling. To avoid condensation on the surface of the powder particles, a nitrogen carrier gas was purged at a flow rate of 50 ml/min. The onset- (T_{gi}), mid- (T_{gm}) and end-point (T_{ge}) values of the mango powders was determined by finding the vertical shift in the heat flow-temperature diagram. All measurements were performed in duplicate.

2.6. Comparison of measured sticky-point temperature with published literature

The sticky-point temperature curves of RW-dried mango powder obtained at different water content using the proposed method were compared with other published sticky-point temperatures of sugar-rich powders such as mango powder (Jaya and Das, 2009), orange juice powder (Brennan et al., 1971), and tomato juice powder (Lazar et al., 1956). The samples with water content ranging from 0.003 to 0.067 kg water/kg dry solids were plotted and superimposed with the existing published data.

3. Results and discussion

3.1. Fundamental basis for characterizing T_s using rheological method

The assumption in characterizing sticky point temperature of the material focused on particle-to-particle stickiness or 'cohesion' and was independent of the types of wall surfaces, e.g. particle-to-wall stickiness or 'adhesion'. The parallel serrated 'groove surface' geometry used in the experiment was considered as a design criterion for the measurements to prevent any mobility at the interface between the plates and the loaded samples. In such conditions, it was assumed that resistance to particle mobility happens only in the interface between the surfaces of the individual particles.

When applying the proposed rheological method to characterize sticky point temperature, we considered the powder sample as a viscoelastic material by means of the measured storage modulus (G') and loss modulus (G''). The presupposition to determine viscoelastic response for food powders where G' is higher than G'' (solid-like) was adopted as a valid reciprocal of the viscoelastic response in food gel where G'' is higher than G' (liquid-like), as reported by Tabilo-Munizaga and Barbosa-Canovas, 2005. Fig. 3a,b,c,d,e,f illustrate the relationships between the G' and the G''. The intersection or *crossover* that may be observed between G' and G'' over a range of temperatures was proposed as the criterion for characterizing the sticky point temperature of the material.

As presented in Fig. 2, we postulated that when the model powder was in its glassy/dry amorphous state, the surfaces of individual particles do not cohere with each other, and hence the

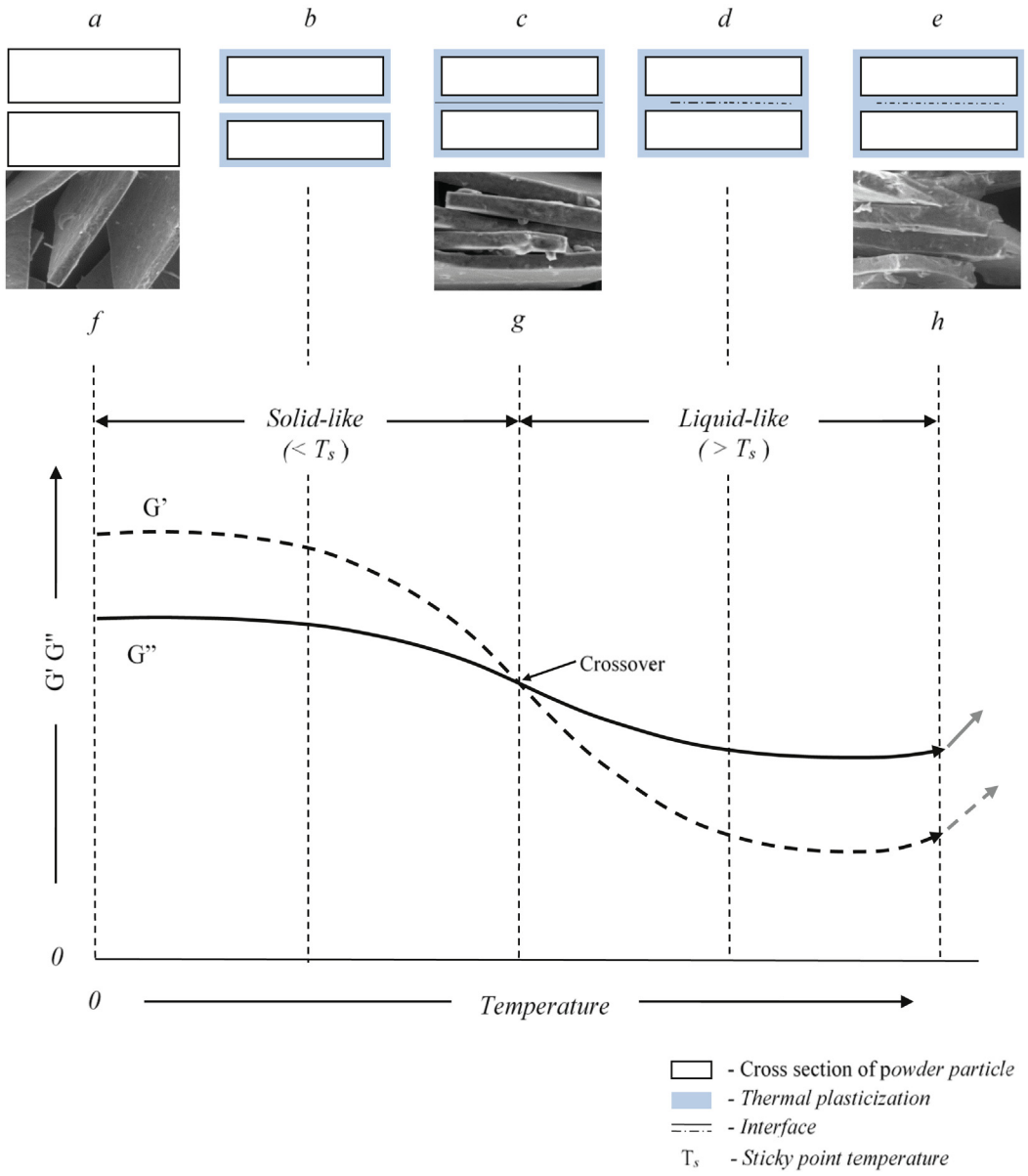

Fig. 2. Proposed mechanism of sticking of sugar-rich amorphous fruit powders applying storage modulus (G′) and loss modulus (G″) concept. Letters (a) to (h) are as previously explained and phase angle between G′ and G″ are for illustration purposes.

materials are free flowing. It can be seen that at the onset of the measurement (a), the values of G' of the powder sample was higher than G'' or the material behaves like a solid, indicating a negligible liquid-bridging or inter-particle forces. The dominance of G' against G'' was due to high surface viscosity of sugar-rich material such as mango powder in its glassy form. This assumption is supported in the study of Downton et al. (1982) who reported that fruit powders containing high sugars have very high viscosity at the glassy stage. White and Cakebread (1966) also stated that amorphous solids are often considered to be "metastable supercooled liquids" below their glass transition temperature with extremely high viscosity in the order of 10^{12} Pa s. When the particles are exposed to higher temperature, their surfaces start to plasticize (b) [thermal plasticization, Roos (2003)], while the difference between the values of G' and G'' decreases. When those solid particles are further heated up, they attract each other and behave more like a "rubbery" liquid with lower viscosity (Downton et al., 1982) until a certain temperature is reached where the two moduli intersect, creating a *crossover*. The lowering of viscosity at this stage allows for a liquid bridging between particles, and hence the powder starts to become sticky and to cohere or adhere to each other (c). When advancing the temperature above the *crossover* point, a reversal of viscoelastic response is observed where G'' becomes dominant over G', suggesting a steady sticky condition of the sample (d & e). Further increase in temperature may result in loss of the stability of particle shape and structure, resulting in cake formation and, finally, in melting of the material. This sticking mechanism that is being postulated is similar to the one reported by other authors based on the expanded caking mechanism as described by Peleg (1983) and Palzer and Sommer (2011).

Other observations may support further explanations about the above presumptions. The sticking phenomena is attributed to

inter-particle attraction as affected by moisture and temperature, either by electrostatic force, liquid bridges, solid bridges or mechanical interlocking (Adhikari et al., 2001). Downton et al. (1982) reported a mechanistic model suggesting that when two moistened particles come in contact, they build a bridge between them that is sufficient to overcome subsequent mechanical deformation leading to reduction of viscosity and hence stick to one another. Specifically, when an initial dry amorphous particle is exposed to higher temperature, its flowability diminishes (Wallack and King, 1988). Due to sensitivity of the amorphous material towards water, the water that diffused from the internal core of the powder particles driven by the rise in temperature may promote steric effects, leading to the development of liquid-bridges (Provent et al., 1993). Once liquid-bridges are developed, the powder begins to transform from its glassy state to a rubbery state, making them to be more sticky and non-flowable (Ozkan et al., 2002). From the above premise, we can state that cohesiveness and stickiness of food powders (over a range of temperatures) are influenced by the formation of liquid-bridging and lowering of material viscosity as defined by the behavior of the G' and G''.

3.2. Storage and loss modulus - time profile as it relates to sticky point temperature

The storage (G') and loss (G'') modulus profiles of the samples as a function of time was established to determine the end-point and average values of the two moduli. The value of G' represents the energy stored in a viscoelastic mass when a strain is applied, while G'' indicates the viscous behavior of the samples that leads to the dissipation of the mechanical energy into heat (Hernandez et al., 2006). The typical plots of G' and G'' at each incremental temperature within the temperature range between 25 and 95 °C are presented in Fig. 3. At the onset temperature of 25 °C for a given sample with specific water content, the G' values recorded for 180 s holding time were always higher than G''. This indicates that the solid-like behavior of the material at this point was discernible. Although both G' and G'' follow a similar path, the difference between the two moduli widened with oscillation time. Ramping the temperature to 35 °C reduced the difference between values of G' and G''. We observed that at the moment the temperature was ramped to 45 °C, differences between the two parameters narrowed even further until a certain point where G'

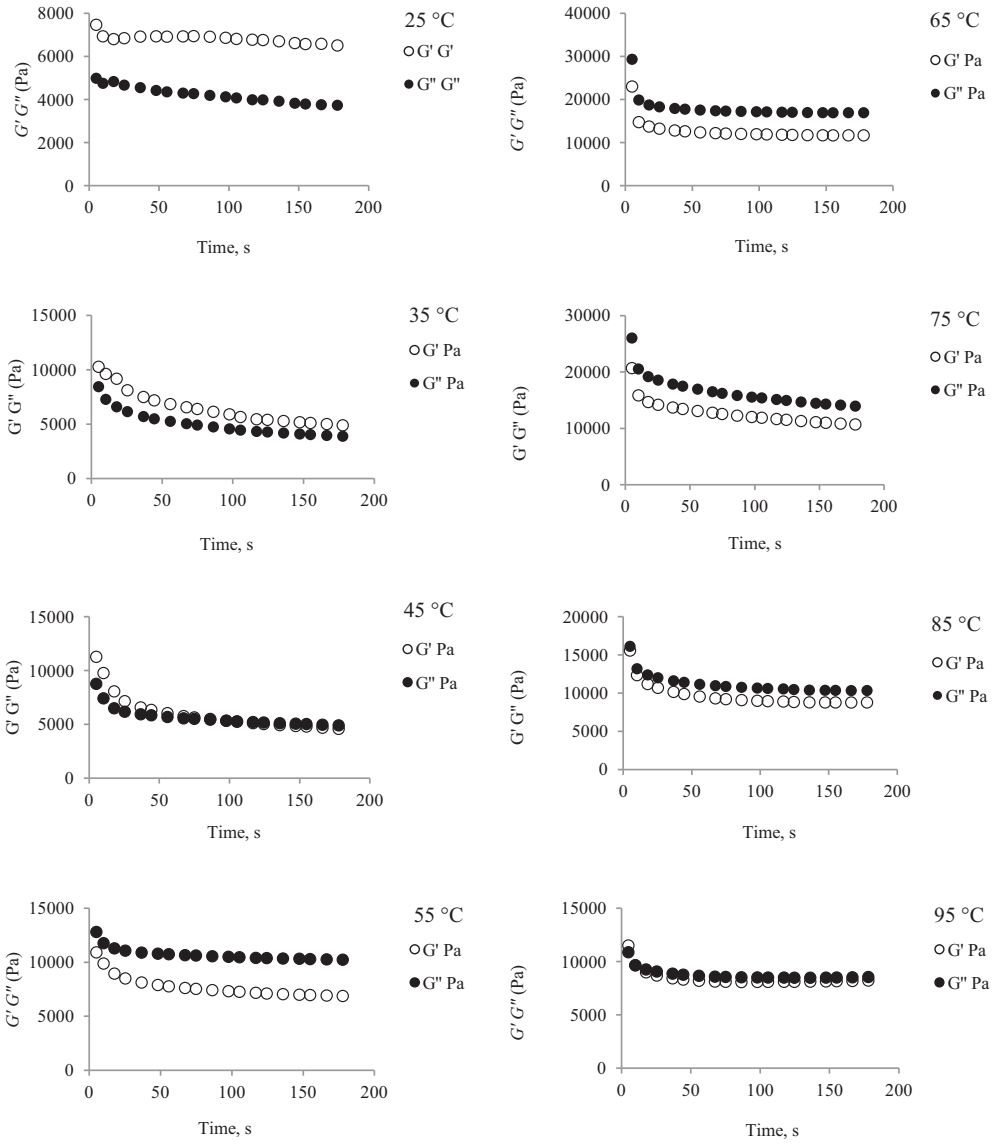

Fig. 3. Typical rheological profile of loss and storage modulus versus time of samples from 25–90 °C at a ramping increment of 10 °C.

Table 1
End- (T_{se}) and Average- (T_{sa}) sticky point temperature of RW-dried mango powder with particle size 180 μm and 500 μm.

Particle size, μm	Water content, kg water/kg dry solids	T_{se}, °C	T_{sa}, °C
180	3.9 ± 0.07	35.40 ± 0.80	36 ± 0.33
500	3.9 ± 0.07	35.87 ± 0.18	39 ± 0.67

and G'' curves intersected and eventually G'' values became higher than G'. When the temperature was ramped to 55 °C and further up to 95 °C, the values of G'' were higher, suggesting that the material remains in a sticky condition. Depending on the water content of the initial samples and particle size, the magnitude of the two moduli may appear interchangeably.

3.3. Sticky-point temperature of mango powder using rheometer method

RW-dried mango powder with particles sizes ranging from 180 to 350 μm (prepared as earlier described) was used for measuring the sticky point temperature at different water content (0.003, 0.022, 0.029, 0.039, 0.048, and 0.067 kg water/kg dry solids). The change in sticky point temperature for the powders within that particle size range was insignificant. This is evident in the preliminary experiments comparing the end- and average-sticky point temperatures of mango powder with particles sizes of 180 and 500 μm (Table 1, Fig 4). The oscillatory testing at 1 Hz (with minimal particle slippage on the serrated parallel plates) facilitates the measurement of infinitesimal disturbances within the particle-to-particle liquid or solid bridges.

Representative graphical plots of G' and G'' as a function of temperature (ranging from 25 to 95 °C) and at those different water contents are shown in Fig. 5 (a to f). Average values from three (3) replicates are summarized in Table 2. It can be seen from the figures that an inverse relationship exists between the sticky point temperature and water content. For example, the measured T_{se} at the lowest water content samples (0.003 kg water/kg dry solids) as shown in Fig. 5a was 83.8 ± 0.8 °C, while the T_{se} at highest water content (0.067 kg water/kg dry solids) as presented in Fig. 5f was 26.3 ± 0.6 °C. A similar trend was observed for the values for T_{sa}.

Overall, the T_{sa} values were found to be higher than T_{se} by 2.3–11.7 °C over a specified range of water content. This result could be attributed to the large variation of G' and G'' values from the start to the last data point during the 180 s holding time at each temperature setting. Using the end-point value when the samples were nearly at steady state condition or thermal equilibrium (Fig. 3) resulted in lower T_{se} values. It is interesting to note that regardless of the differences in magnitude of G' and G'', which could be attributed to slight variations during loading and sample packing density (e.g., shown in Fig. 5), the intersection or *crossover* (denoted as the sticky point temperature) observed from the G' and G'' curves was very consistent with a high degree of repeatability (SD = 0.58–1.73 °C). This suggests that the temperature at which the *crossover* occurs is independent of the magnitude of G' and G'' values.

3.4. Relationship between sticky-point and glass transition temperatures

The experimental values obtained from the current investigation for sticky point and glass transition temperatures between

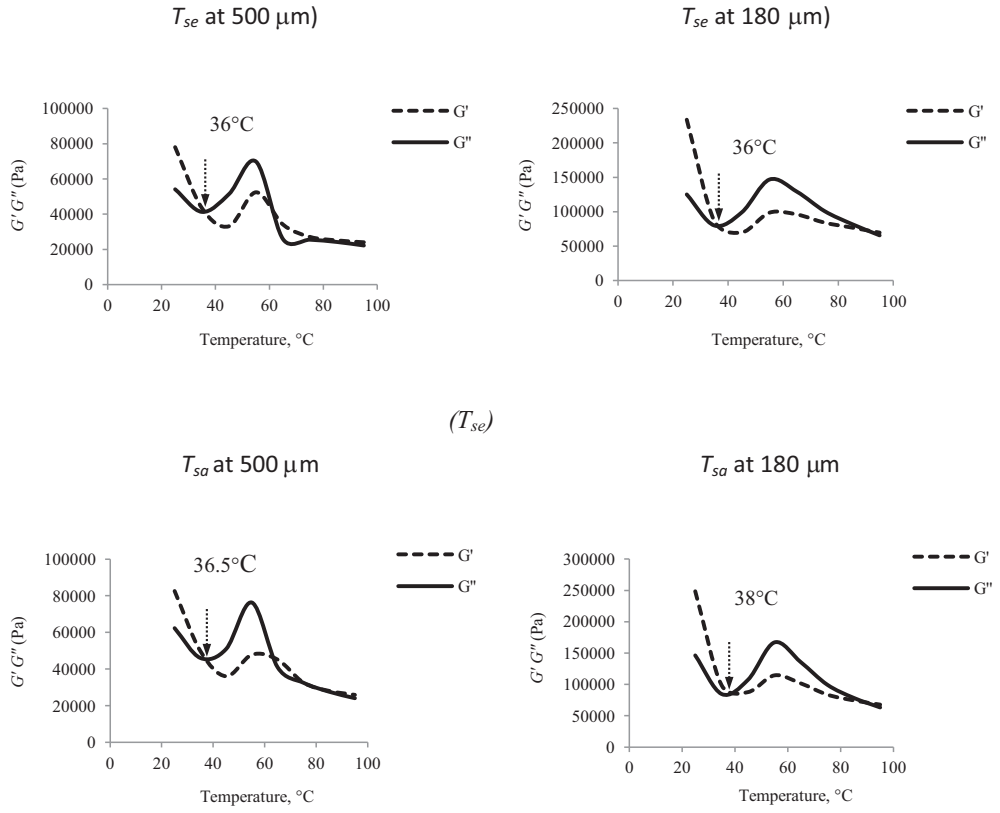

Fig. 4. Representative graphical plot of end-point sticky point temperature (T_{se}) and Average sticky point temperature (T_{sa}) of RW-dried mango powder at 180 and 500 μm particle size and water content of 0.039 kg water/kg dry solids.

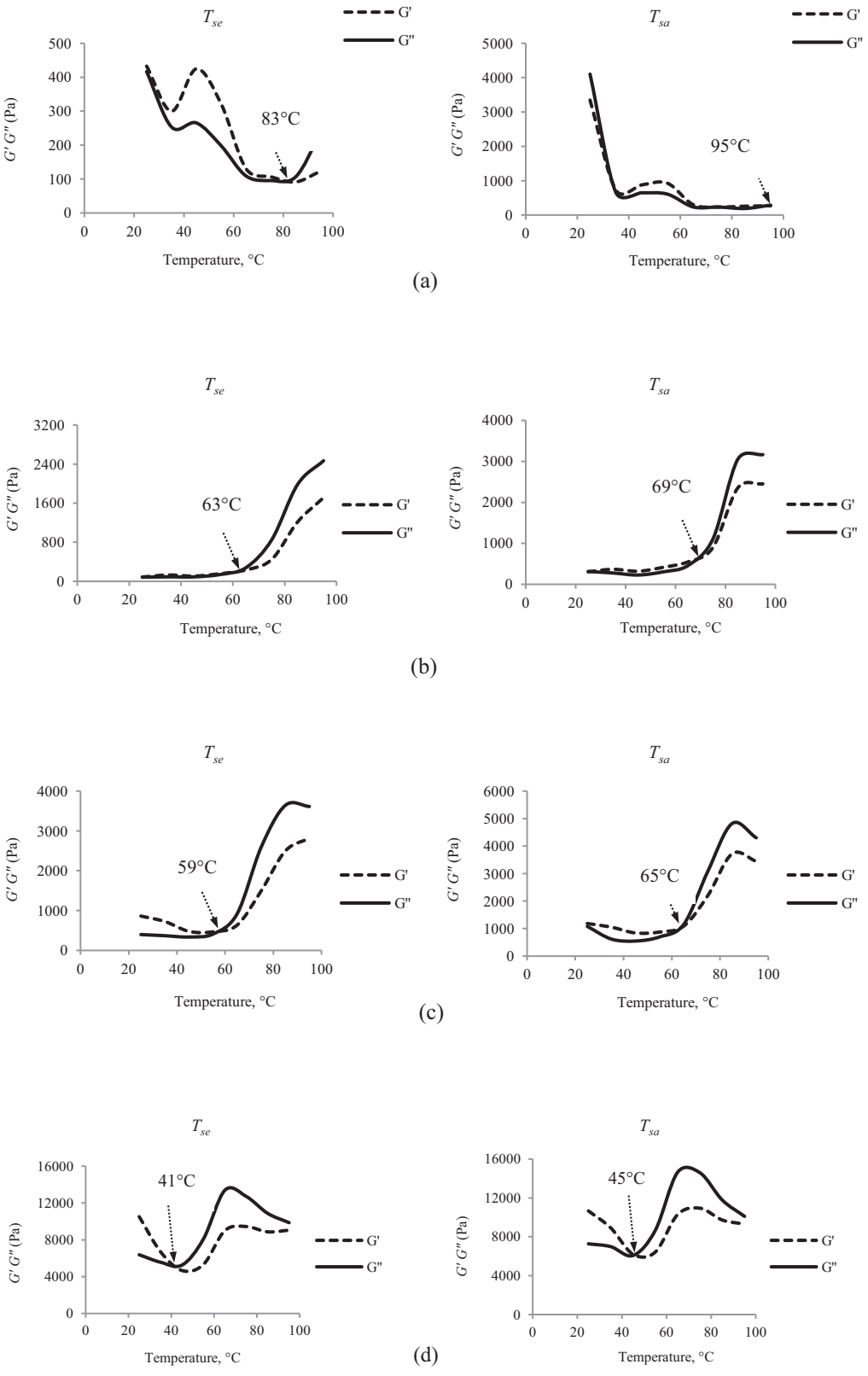

Fig. 5. Representative graphical plot of end-point (T_{se}) and average (T_{sa}) sticky point temperature of samples equilibrated at water content of (a) 0.003, (b) 0.022, (c) 0.029, (d) 0.039, (e) 0.048, and (f) 0.067 kg water/kg dry solids.

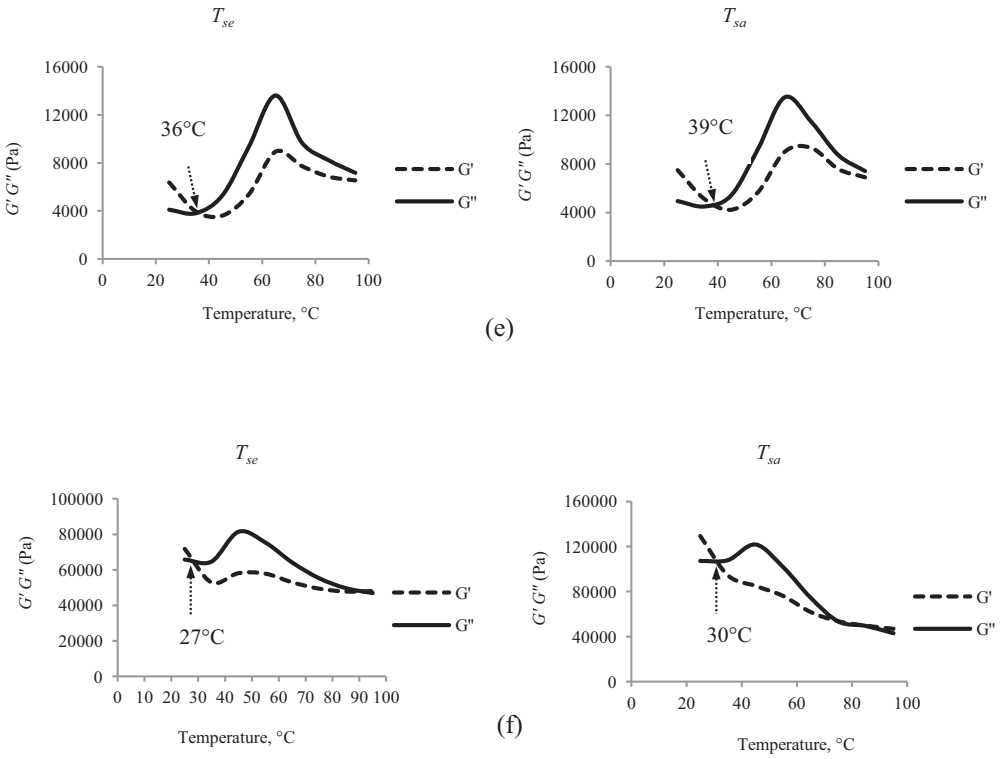

Fig. 5. (*continued*).

the lower and higher water contents showed a high degree of linearity with a coefficient of determination (R^2) ranging from 0.91 to 0.97 (Fig. 6). As is evident in the figure, the sticky point temperatures (T_{se} and T_{se}) of mango powder was always higher than the glass transition temperature (T_g) at different water content. Previous investigations by Roos and Karel (1991b) and Jaya and Das (2009) showed that there was a linear relationship between sticky point temperature (T_s) and glass transition temperature (T_g) of sugar-rich materials at different water contents. The proposed method to describe the sticky phenomenon (as presented in Fig. 6) strongly supports those findings. Both of these temperatures decrease with the increase in water content - a pattern which is typical of the plasticization effect of water in suppressing the glass transition temperature of amorphous solids (Slade and Levine, 1991). Similar behavior was reported by Roos and Karel (1991a) on the effect of water plasticization on amorphous sucrose-fructose model foods. At the lowest water content of 0.003 kg water/kg dry solids, the T_{se} and T_{se} were 83.83 ± 0.56 °C and 95.00 ± 0.11 °C, respectively. On the other hand, the onset (T_{gi}), mid- (T_{gm}) and end- (T_{ge}) glass transition temperature of the same samples was recorded at 49.15 ± 0.55, 51.30 ± 0.44 °C and 54.00 ± 0.20 °C, respectively. At the higher water content of 0.067 kg water/kg dry solids, the values of T_{se} and T_{sa} were reduced to 26.33 ± 0.44 °C and 29.67 ± 0.44 °C, respectively, with corresponding T_{gi}, T_{gm} and T_{ge} of −4.00 ± 1.70 °C, −3.95 ± 1.76 °C and −0.57 ± 1.32 °C. The differences between T_{se} versus T_{gi}, T_{gm} and T_{ge} was calculated to be 21–44 °C, while a higher range difference of 25–50 °C was observed between T_{sa} versus T_{gi}, T_{gm} and T_{ge} (Table 3). These variations are attributed to the lower values of T_{se} compared to the average of data points calculated for T_{sa}. The sticky point temperature was 4–11 °C higher than glass transition temperature in sucrose: fructose (87.5:12.5% w/w mixture) (Downton et al., 1982), 11.5–15.5 °C for vacuum dried mango powder with

Table 2
Water content, sticky point temperature adapting the new rheometric method and glass transition temperature of mango powder at different water content.

No.	Water content, kg/kg dry solids	Sticky point temperature		Glass transition temperature		
		T_{se}	T_{sa}	T_{gi}	T_{gm}	T_{ge}
1	0.003 ± 0.001	83.83 ± 0.56	95.00 ± 0.11	49.15 ± 0.55	51.30 ± 0.44	54.00 ± 0.20
2	0.022 ± 0.008	64.00 ± 0.67	69.67 ± 0.44	20.45 ± 0.05	23.10 ± 0.20	26.85 ± 0.45
3	0.029 ± 0.003	58.50 ± 1.00	66.00 ± 1.33	15.60 ± 0.20	19.10 ± 0.30	23.55 ± 0.35
4	0.039 ± 0.007	41.33 ± 1.11	44.67 ± 1.11	12.60 ± 0.20	16.20 ± 0.10	19.95 ± 0.05
5	0.048 ± 0.003	35.67 ± 0.44	38.00 ± 0.67	2.00 ± 0.10	5.20 ± 0.10	8.65 ± 0.05
6	0.067 ± 0.008	26.33 ± 0.44	29.67 ± 0.44	−4.00 ± 1.02	−3.95 ± 0.76	−0.57 ± 1.32

1 Samples were stored in P_2O_5 for 30 days.
2 Reference sample was oven-dried for 1 h at 50 °C.
3 Reference RW-dried mango powder was oven-dried for 30 min at 50 °C.
4 Reference RW-dried mango powder with water content of 3.89 kg water/kg dry solids.
5 Reference RW-dried mango powder conditioned for 20 min inside a desiccator at 100% RH.
6 Reference RW-dried mango powder conditioned for 40 min inside a desiccator at 100% RH.

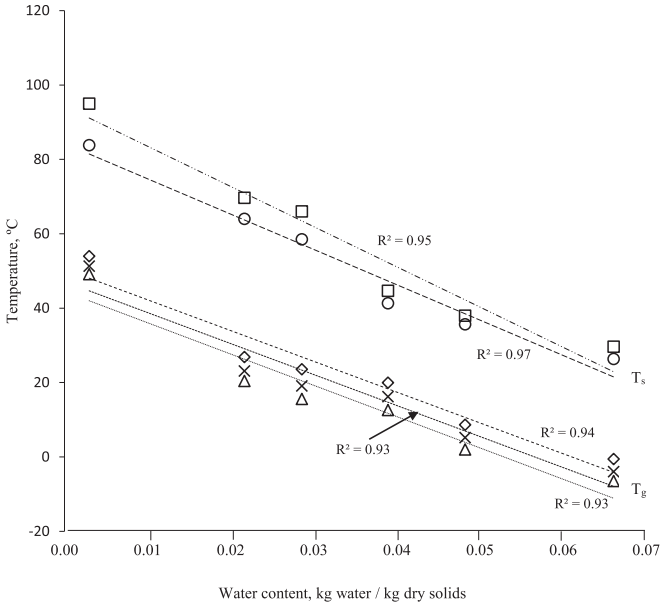

Fig. 6. Relationship of sticky point temperature and glass transition temperature of RW-dried mango powder as function of water content. [T_{se} (○); T_{sa} (□); T_{gi} (△); T_{gm} (×); Tge (◇)].

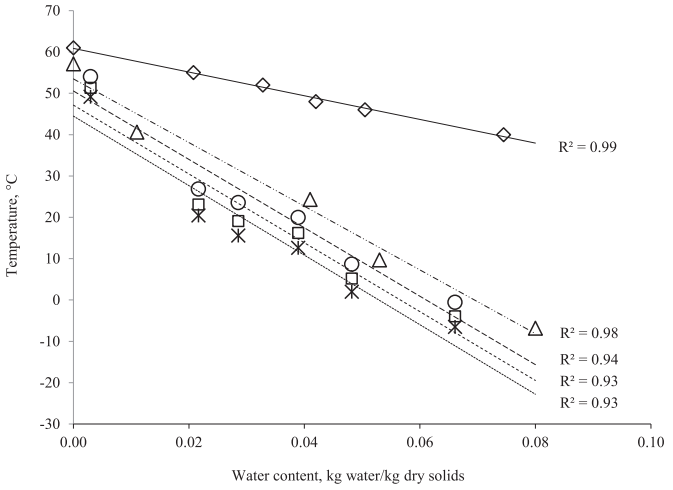

Fig. 7. Comparison of glass transition temperature of sucrose-fructose model food, RW-dried, and vacuum-dried mango powders. [△ – Sucrose-fructose (7:1), (Roos & Karel, 1991b); * T_{gi}, □ – T_{gm}, and ○ – T_{ge} of RW-dried powder without additives (present study); ◇ Vacuum-dried mango powder + maltodextrin (Jaya & Das, 2009)].

0.093 kg maltodextrin/kg dry solids, 2.5–3.5 °C for pineapple with 0.065 kg maltodextrin/kg dry solids (Jaya and Das, 2009), and 10–20 °C for mixtures of amorphous sucrose-fructose sugars (7:1 ratio) (Roos and Karel, 1991a). The data on sticky point and glass transition temperatures of model fruit powder over the range of water contents investigated is in agreement with those previous studies.

The higher range of differences between sticky point temperature and glass transition temperature obtained from the current investigation (25–50 °C) in comparison with the combined data obtained from the literature cited above (4–20 °C) could be attributed to various factors including variations of chemical composition (e.g. sugar content) and molecular weight of fruit components used, drying method, water content measurement method (oven versus Karl Fisher), powder particle size, and surface structure of the dried product. The methods applied in measuring the sticky point temperature for each product could also influence these variations. Although either of the T_{se}, T_{sa} and T_g obtained in the present study are higher than those in previous reports, our results clearly revealed that a defined constant range of differences between the two temperatures ($T_s - T_g$) existed within a given range of water content. The measurements obtained were very consistent and repeatable (SD = 0.58–1.73 °C, greater than 98% precision).

3.5. Comparison of T_g of RW-dried mango powder with published data

The T_g values of vacuum-dried mango powder with 0.093 kg maltodextrin, DE 36/kg dry solids (Jaya and Das, 2004) and a sucrose: fructose powder (7:1 ratio) (Roos and Karel, 1991a) were compared to the T_g of RW-dried mango powder investigated (Fig. 7). It was observed that the T_g of vacuum-dried mango powder tended to be greater than that of RW-dried mango powder and sucrose: fructose model powder over a range of water content (e.g. 0–0.075 kg water/kg dry solids). This apparent trend is most likely due to the higher glass transition temperature (T_{gs} = 100 °C) of maltodextrin (DE 36) that was added to the vacuum-dried powder, in contrast to sucrose: fructose powder (T_{gi} = 57.1 and T_{ge} = 68 °C) (Roos and Karel, 1991a) and RW-dried mango powder (T_{gs} = 55.8 °C) (Caparino et al., 2012) (Table 4). It is known that adding a high molecular weight polysaccharide such as maltodextrin to a low molecular weight material raises the T_g of the latter

Table 3
Differences between the sticky point temperature and glass transition temperature of mango powder at different water content.

Water content, kg/kg dry solids	Difference ($T_s - T_g$), °C					
	$T_{se} - T_{gi}$	$T_{se} - T_{gm}$	$T_{se} - T_{ge}$	$T_{sa} - T_{gi}$	$T_{sa} - T_{gm}$	$T_{sa} - T_{ge}$
0.003 ± 0.001	35	33	30	46	44	41
0.022 ± 0.008	44	41	37	49	47	43
0.029 ± 0.003	43	39	35	50	47	42
0.039 ± 0.007	29	25	21	32	28	25
0.048 ± 0.003	34	30	27	36	33	29
0.067 ± 0.008	30	30	27	34	34	30
Differences	29–44	25–41	21–37	32–50	28–47	25–43

T_s-Sticky point temperature.
T_g-Glass transition temperature.
T_{se}-End-point sticky point temperature.
T_{sa}-Average-point sticky point temperature.
T_{gi}-Onset glass transition temperature.
T_{gm}-Mid-point glass transition temperature.
T_{ge}-End-point glass transition temperature.

Table 4
Glass transition temperatures of selected fruits, anhydrous sugars and carbohydrate polymers.

Product	T_{gs}, °C	Melting point, °C	Sucrose, kg/kg pulp (%)	Glucose, kg/kg pulp (%)	Fructose, kg/kg pulp (%)	Organic acid, kg/kg pulp (%)	References
Mango							
- RW-dried	55.8	–	–	–	–	–	Caparino et al., 2012
- Freeze-dried	63.6	–	–	–	–	–	Caparino et al., 2012
- Vacuum-dried	61	–	0.064	0.047	0.026	0.003	Jaya and Das, 2009
Pineapple - Vacuum-dried	61	–	0.062	0.037	0.016	0.002	Jaya and Das, 2009
Orange							
- Without carrier	5.7	–	(43.1)	–	–	(43.1)	Goula and Adamopolous, 2010
- With DE 6[a] maltodextrin (50:50)	66	–	(48–52)	–	–	(5.3–6.3)	Goula and Adamopolous, 2010
- With DE 6 maltodextrin (50:50)	78	–	(43.1)	–	–	(4.3)	
Tomato	31	–	0.006	0.010	0.010	0.006	Bhandari et al., 1997; Jaya and Das, 2009
Amorphous food model Sucrose-Fructose (7:1)	57	–	–	–	–	–	Roos and Karel, 1991b
Sucrose-Fructose solution (87.5: 12.5%) mixture	–	–	(87.5)	–	(12.5)	–	Downton et al., 1982
Sucrose	62	–	–	–	–	–	Jaya and Das, 2009
	–	173	–	–	–	–	Roos, 1993
D-Glucose	31	–	–	–	–	–	Jaya and Das, 2009
	–	163	–	–	–	–	Roos, 1993
D-Fructose	5	–	–	–	–	–	Jaya and Das, 2009
	–	108	–	–	–	–	Roos, 1993
Organic acid	11	–	–	–	–	–	Jaya and Das, 2009
	–	153	–	–	–	–	Roos, 1993
Starch	250	–	–	–	–	–	Roos, 2003
Maltodextrin							
DE 5	188	240	–	–	–	–	Roos and Karel, 1991b
DE 10	160	–	–	–	–	–	Roos and Karel, 1991b
DE 20	141	–	–	–	–	–	Roos and Karel, 1991b
DE 36	100	–	–	–	–	–	Roos and Karel, 1991b

[a] DE: Dextrose equivalents.

(Jaya and Das, 2004). The slight deviation in the T_g of sucrose: fructose model and RW-dried mango powders could be attributed to similar amount of sugar in both products.

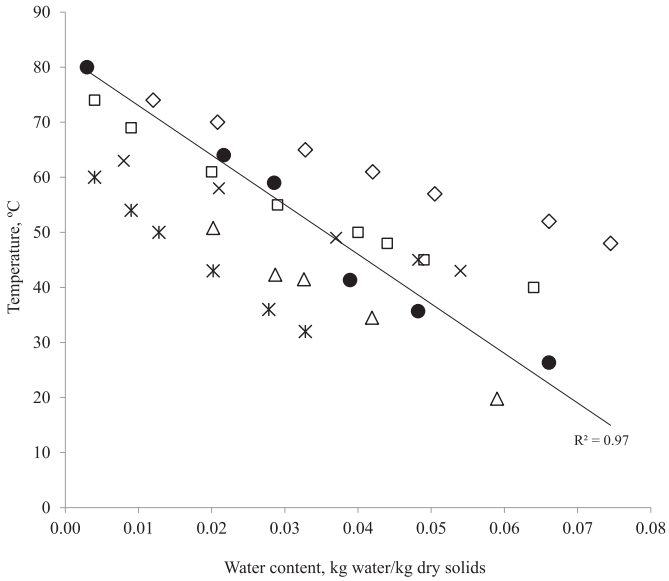

Fig. 8. Sticky point temperatures of RW-dried mango powder and other sugar-rich fruit powders. [● RW-dried mango powder without additives (present study); ◇ Vacuum-dried mango powder + 0.093 kg maltodextrin/kg of pulp (Jaya & Das, 2009); △ Sucrose-fructose powder (Downton et al., 1971); × Pineapple juice powder + 0.065 kg maltodextrin/kg of pulp (Jaya & Das, 2009); * Orange juice powder + liquid glucose, 39-43 DE (Brennan et al, 1971); □ Tomato powder (Lazar et al., 1956)].

3.6. Comparison of measured sticky-point temperature with published data

The sticky point temperature of RW-dried mango powder measured using the rheometer (Fig. 8) was compared with those of other sugar-rich fruit powders measured by a sticky-point tester developed by Lazar et al. (1956). The sticky point temperature of the RW-dried mango powder decreased with increase in water content and that trend is similar to the measured glass transition temperatures. This inverse relationship of T_s versus water content is similar for other food powders such as vacuum-dried mango and pineapple juice powder (Jaya and Das, 2009), orange juice powder (Brennan et al., 1971), model powder containing sucrose: fructose (Downton et al., 1982), and tomato juice powder (Lazar et al., 1956). Fig. 8 indicates that the sticky point temperature measured using the new method is within the range of experimental values obtained for the different fruits mentioned. Evidently, the orange juice powder showed the lowest sticky point temperature among the other products presented. One possible reason for this is the low T_s of orange juice powder without a carrier, which measured only 5.7 °C (Goula and Adamopolous, 2010). Although liquid glucose was added during the processing of orange juice powder, the lower T_s obtained is justified because this sugar has low T_g of 31 °C (Table 4). This is far below the T_g of mango powder without a carrier obtained by RW drying (T_{gs} = 55.8 °C) and freeze drying (T_{gs} = 63.6 °C) methods, as reported by Caparino et al. (2012). On the other hand, the sticky point temperature of the vacuum-dried mango powder is higher compared to that of RW-dried counterpart because maltodextrin was added to it. The sticky point temperature of RW-dried mango powder showed little variation compared to the sucrose: fructose (87%: 12.5%) mixture, which could also be attributed to similar sugar concentration of the product.

The new proposed method for determining the sticky point temperature based on advanced controlled stress – strain rheometer with a special serrated parallel plate geometry is more accurate and precise when compared to the device developed by Lazar et al. (1956). This claim is justified because, unlike the latter method, which applied human perception or feeling by hand, the present method is automated and uses computer software to generate data directly from a rheometer that provides both controlled stress and strain data. In addition, the sample preparation is standardized and carefully managed, a procedure which adds consistency and reliability for this new method.

4. Conclusions

The results of the experimental investigation clearly demonstrate that the new proposed rheometer method is suitable as an alternative technique to quantify and characterize sticky point temperature of sugar-rich powder materials. A crossover between the storage modulus (G') and loss modulus (G'') of a powder product was established and denoted as sticky point temperature of RW-dried mango powder at different water content. The data obtained using the new method was highly correlated to the glass transition temperature of the product. A direct relationship between the sticky point and glass transition temperatures of RW-dried mango powder agreed with other published sugar-rich powder materials. The developed procedure and protocol for sample conditioning and rheometric measurement to determine the sticky point temperature of the material is easy to implement. The new technique can measure the sticky point temperature of a food powder with a high degree of repeatability, reliability, and accuracy. While there is strong evidence to support this, more experiments using the new developed method are needed to further confirm its application to a wider range of food powders. Measuring the crystallization and melting point of fruit powders and obtaining additional data to gain more understanding of other theoretical aspects of the sticky point phenomena using the proposed method is recommended.

Acknowledgments

We thank the Ford Foundation International Fellowship Program (IFP)/Institute of International Education (IIE)-New York through the IFP - Philippine Social Science Council (IFP-PSSC) for providing financial support (Grant #15067041); the Philippine Center for Postharvest Development and Mechanization (PhilMech) for granting study leave to first author. Wayne Dewitt for helping in the fabrication of the powder loading device, and Binying Ye for providing technical assistance on the operation of advanced rheometer, DSC and Karl Fisher Moisture Tester.

References

Adhikari, B., Howes, T., Bhandari, B., Truong, V., 2003. In situ characterization of stickiness of sugar-rich foods using a linear actuator driven stickiness testing device. J. Food Eng. 58, 11–22.
Adhikari, B., Howes, T., Bhandari, B.R., Truong, V., 2001. Stickiness in foods: a review of mechanisms and test methods. Int. J. Food Prop. 4 (1), 1–33.
Barbosa-Canovas, G.V., Ortega-Rivas, E., Juliano, P., Yan, H. (Eds.), 2005. Food Powders: Physical Properties, Processing, and Functionality. Kluwer Academic/Plenum Publishers, New York, NY.
Bhandari, B.R., Datta, N., Howes, T., 1997. Problems associated with spray drying of sugar-rich foods. Dry. Technol. 15 (2), 671–684.
Boonyai, P., Bhandari, B., Howes, T., 2004. Stickiness measurement techniques for food powders: a review. Powder Technol. 145, 34–46.
Brennan, J.G., Herrera, J., Jowitt, R., 1971. A study of some of the factors affecting the spray drying of concentrated orange juice on a laboratory scale. J. Food Technol. 6 (3), 295–307.
Caparino, O.A., Tang, J., Nindo, C.I., Sablani, S.S., Powers, J.R., Fellman, J.K., 2012. Effect of drying methods on the physical properties and microstructures of mango (Philippine 'carabao' var.) powder. J. Food Eng. 111, 135–148.
Dixon A., Bloore C., & Rhodes M. (1999). Correlating food powder stickiness with composition, temperature, and relative humidity.
Downton, G.E., Flores-Luna, J.L., King, C.J., 1982. Mechanisms of stickiness in hygroscopic, amorphous powders. Ind. Eng. Chem. Fundam. 21, 447–451.
Goula, A.M., Adamopolous, K.G., 2010. A new technique for spray drying orange juice concentrate. Innov. Food Sci. Emerg. Technol. 11 (2), 342–351.
Goula, A.M., Karapantsios, T.D., Adamopoulos, K.G., 2007. Characterization of tomato pulp stickiness during spray drying using a contact probe method. Dry. Technol. 25, 591–598.
Green, H., 1941. The tackmeter, an instrument for analyzing and measuring tack. Ind. Eng. Chem. Anal. 13, 632–639.
Hennigs, C., Kockel, T.K., Langrish, T.A., 2001. New measurements of the sticky behavior of skim milk powder. Dry. Technol. 19 (3–4), 471–484.
Hernandez, L., Gurruchaga, M., Goni, I., 2006. Influence of powder particle size distribution on complex viscosity and other properties of acrylic bone cement for vertebroplasty and kyphoplasty. J. Biomed. Mater. Res. Part B Appl. Biomater. 77B (1), 98–103.
Jaya, S., Das, H., 2009. Glass transition and sticky point temperatures and stability/mobility diagram of fruit powders. Food Bioprocess Technol. 2, 89–95.
Jaya, S., Das, H., 2004. Effect of maltodextrin, glycerol monostearate and tricalcium phosphate on vacuum dried mango powder properties. J. Food Eng. 63, 125–134.
Jenike, A.W., 1964. Storage and flow of solids. In: Engineering Experimental Station, vol. 123. University of Utah, Utah.
Kilcast, D., Roberts, C., 1998. Perception and measurement of stickiness in sugar-rich foods. J. Texture Stud. 29, 81–100.
Kudra, T., Mujumdar, A.S., 2002. Advanced Drying Technologies. Marcel Dekker, Inc., New York.
Lazar, W.E., Brown, A.H., Smith, G.S., Wong, F.F., Lindquist, F.E., 1956. Experimental production of tomato powder by spray drying. Food Technol. 10 (3), 129–134.
Menjivar, J.A., Faridi, H., 1994. Rheological properties of cookie and cracker doughs. In: Faridi, H. (Ed.), The Science of Cookie and Cracker Production. Chapman & Hall, New York, pp. 283–322.
Mezger, T.G., 2006. The Rheology Handbook: for Users of Rotational and Oscillatory Rheometers. Vincentz Network GmbH & Co KG.
Ozkan, N., Walisinghe, N., Chen, X.D., 2002. Characterization of stickiness and cake formation in whole and skim milk powders. J. Food Eng. 55, 293–303.
Palzer, S., Sommer, K., 2011. Caking of water-soluble amorphous and crystalline food powders. In: Aguilera, J.M., Simpson, J., Welti-Chanes D, B., et al. (Eds.), Food Engineering Interfaces. Springer, New York, pp. 419–514.
Paterson, A.H., Bronlund, J.E., Brooks, J.F., 2001. The blow test for measuring the stickiness of powders. In: AIChE 2001 Annual Meeting, Reno, NV.
Peleg, M., 1983. Physical characteristics of food powders. In: Peleg, M., Bagley, E.B. (Eds.), Physical Properties of Foods. AVI Publishing Co, Westport, CT, pp. 293–323.
Provent, B., Chulia, D., Cary, J., 1993. Particle size and the caking tendency of a powder. Eur. J. Pharm. Biopharm. 39 (5), 2002–2007.
Rao, M.A., 1999. Rheological behavior of processed fluid and semisolid foods. In: Rao, M.A. (Ed.), Rheology of Fluid and Semisolid Foods: Principles and Operations. Springer Science & Business Media, pp. 105–108; 244-254.
Roos, Y.H., 2003. Thermal analysis, state transition and food quality. J. Therm. Anal. Calorim. 71 (1), 197–203.
Roos, Y.H., 1993. Water activity and physical state effects on amorphous food stability. J. Food Process. Preserv. 16, 433–447.
Roos, Y.H., Karel, M., 1991a. Plasticizing effect of water on thermal behavior and crystallization of amorphous food models. J. Food Sci. 56, 38–43.
Roos, Y.H., Karel, M., 1991b. Phase transitions of mixtures of amorphous polysaccharides and sugars. Biotechnol. Prog. 7, 49–53.
Schubert, H., 1987. Food particle technology. Part I: properties of particles and particulate food systems. J. Food Eng. 6 (1), 1–32.
Slade, L., Levine, H., 1991. A food polymer science approach to structure-property relationships in aqueous food systems: non-equilibrium behavior of carbohydrate-water systems. In: Levine, H., Slade, L. (Eds.), Water Relationships in Foods. Plenum Press, New York, pp. 29–101.
Syamaladevi, R.M., Sablani, S.S., Tang, J., Powers, J., Swanson, B.G., 2009. State diagram and water adsorption isotherm of raspberry (*Rubus idaeus*). J. Food Eng. 91 (3), 460–467.
Tabilo-Munizaga, G., Barbosa-Canovas, G.V., 2005. Rheology for the food industry. J. Food Eng. 67 (1), 147–156.
Tsourouflis, S., Flink, J.M., Karel, M., 1976. Loss of structure in freeze-dried carbohydrates solutions: effect of temperature, moisture content and composition. J. Sci. Food Agric. 27, 509–519.
Villa-Rojas, R., Tang, J., Wang, S., Gao, M., Kang, D.H., Mah, J.H., Gray, P., Sosa-Morales, M.E., Lopez-Malo, A., 2013. Thermal Inactivation of *Salmonella Enteritidis* PT30 in almond kernels as influenced by water activity. J. Food Prot. 76 (1), 26–32.
Wallack, D.A., King, C.J., 1988. Sticking and agglomeration of hygroscopic, amorphous carbohydrate and food powders. Biotechnol. Prog. 4 (1), 31–35.
White, G.W., Cakebread, S.H., 1966. The glassy state of certain sugar-containing food products. J. Food Technol. 1, 73–82.